Accepted for publication at the 2026 IEEE PES General Meeting (PESGM), Montréal, QC, Canada.
This is the accepted author manuscript. Copyright transferred to IEEE.
Please cite this work as:
K. Pokharel, M. Ataei, J. L. Diaz, F. Andrade Rengifo, R. Tonkoski, V. Dhiman, and H. Li, "Safe Control of Grid-Following Inverters using Control Lyapunov and Barrier Functions with Stability Guarantees," ***2026 IEEE PES General Meeting (PESGM)*****, Montréal, QC, Canada, 2026.**

Safe Control of Grid-Following Inverters using Control Lyapunov and Barrier Functions with Stability Guarantees

Kajal Pokharel*, Masoud Ataei*, Vikas Dhiman, and Hepeng Li†
Department of Electrical and Computer Engineering
University of Maine
Orono, Maine, USA

Jan L Diaz, Fabio Andrade Rengifo
Department of Electrical and Computer Engineering
University of Puerto Rico
Mayagüez, Puerto Rico, USA

Reinaldo Tonkoski‡
Electric Power Transmission and Distribution
Technical University of Munich
Munich, Germany

***Abstract*—Conventional controllers, such as Proportional-Integral (PI) regulators, used for current regulation, often fail to prevent overshoot during transients, potentially violating inverter current limits and compromising device safety. To address this limitation, this paper presents a unified control framework using Control Lyapunov Functions (CLFs) and Control Barrier Functions (CBFs), which have been well-studied in the control theory literature. The controller is formulated as a CLF-CBF based Quadratic Program (QP), where the CLF guarantees stability of current tracking and the CBF enforces safety constraints limits within a pre-defined safe set. A quadratic program can be solved at a high frequency. The proposed controller is implemented in MATLAB/Simulink and tested on a three phase grid-connected inverter with an LCL filter and compared against the PI, and Linear Quadratic Regulator (LQR) controllers under voltage sag conditions. Across all three controllers, the proposed CLF-CBF controller achieves safe and stable current tracking while reducing the peak current from 237.8 A (PI) and 240.8 A (LQR) to 219.5 A, and lowering total harmonic distortion (THD) from 4.72% (PI) and 5.63% (LQR) to 3.46%.**

***Index Terms*—Grid Following Inverters, Safe Control, Control Lyapunov Function (CLF), Control Barrier Function (CBF), Linear Quadratic Regulator (LQR)**

I. Introduction

Inverter-based resources are increasingly responsible for supporting modern power systems with the rapid integration of distributed energy. Control of these inverters plays a critical role in shaping system stability, dynamic response, and power quality [1]. Research on grid-following inverter control has produced a wide range of strategies to improve transient performance and ride-through capability [2]. Nevertheless, safety remains insufficiently addressed, as many controllers are evaluated mainly on tracking and power-quality metrics and offer little in the way of explicit guarantees on safe operation under severe disturbances and constraints.

Most existing literature focuses on maintaining system stability under disturbances, rather than explicitly enforcing device-level safety. PI controllers in synchronous or stationary frames are widely used for their simplicity and ease of implementation [3], while state-feedback and Linear Quadratic Regulator (LQR) designs exploit system models to improve dynamic response [4], [5]. Model predictive, adaptive, neural-network and other learning-based controllers have been used to improve performance or adaptivity using data, often on top of conventional control structures to enhance performance under uncertainty [6], [7]. Despite their effectiveness in achieving equilibrium, safety is typically addressed indirectly through controller saturation, heuristic current limits, or conservative tuning. In grid following inverters, this often results in large current peaks during faults or rapid operating-point changes, posing significant risks to converters and other connected equipment.

Recently, Control Lyapunov Function (CLF) and Control Barrier Function (CBF) based frameworks have emerged as a principled approach for unifying stability and safety in control systems. In the power systems literature, CLF–CBF methods have been successfully applied to voltage and frequency regulation problems, particularly in grid-forming inverters and microgrids, where they provide formal guarantees on stability, constraint satisfaction, and transient performance [8], [9], [10], [11]. These studies demonstrate the promise of CLF–CBF frameworks for safety-critical power applications. However, their focus has largely remained on outer-loop control problems operating on relatively slow electromechanical or voltage time scales.

In contrast, inner-loop current control of grid-following inverters poses fundamentally different challenges that are not addressed by existing CLF–CBF formulations. First, current control operates on fast electromagnetic time scales, requiring deterministic execution compatible with high-frequency PWM updates. Second, during grid disturbances such as voltage sags, the current reference demanded by outer control loops may become temporarily incompatible with hard current limits, creating an inherent and immediate conflict between tracking and safety. Third, transient overcurrents can develop in a few milliseconds, leaving little margin for corrective action through

*These authors contributed equally to this work. ‡Reinaldo Tonkoski is also an adjunct professor at the University of Maine. This work is supported by the National Science Foundation (NSF) under OIA-2316399, OIA-2218063, and OIA-2316401. †Correspondence: hepeng.li@maine.edu

conventional limiters. Existing CLF–CBF approaches, developed primarily for voltage-source or outer-loop dynamics, do not directly address this fast, safety-critical inner-loop regime.

This paper addresses this gap by proposing a new CLF–CBF based current controller for grid-following inverters that guarantees safe inverter currents while preserving tracking performance. The proposed controller exploits the natural complementarity between CLFs and CBFs where CLFs ensure stability and robustness to disturbances [10], while CBFs enforce safety constraints [12]. By embedding both in a quadratic program, the controller dynamically balances stability and safety objectives in real time [13]. The effectiveness is demonstrated by benchmarking against conventional PI and LQR controllers under transient conditions caused by load and generation fluctuations. The main contributions are summarized as follows:

- A CLF-CBF-based controller is developed for inner-loop current control of grid-following inverters, explicitly enforcing hard current limits during fast electromagnetic transients through a computationally efficient quadratic program with relative-degree-one barrier functions.
- A novel theoretical bound on the CBF parameter γ is derived as a function of switching frequency, and a super-linear barrier function is introduced that allows smoother control away from current limits while maintaining aggressive safety enforcement near boundaries.
- We implement the proposed method and evaluate it against baselines of PI and LQR-based controllers. The proposed CLF-CBF controller achieves safe and stable current tracking while reducing the peak current from 237.8 A (PI) and 240.8 A (LQR) to 219.5 A, and lowering total harmonic distortion (THD) from 4.72% (PI) and 5.63% (LQR) to 3.46%.

II. Problem Formulation

In this section, we consider a grid-following inverter (GFL) that injects controlled active and reactive currents into the grid. The objective is to regulate the inverter-side currents (i_{1d}, i_{1q}) to their reference values (i_d^{ref}, i_q^{ref}) while ensuring that the instantaneous current magnitude remains within a prescribed safe limit. The three-phase grid-connected inverter with an LCL filter used for this study is shown in Fig. 1. The DC-link voltage V_{dc} is converted to three-phase AC voltages $v_{1,abc}$, which are applied to the LCL filter L_1, R_1, C_1, L_2, R_2 and then injected into the grid with line voltages $v_{2,abc}$. The inverter switches s_1-s_6 are modulated by a PWM block. We assume that the DC-link voltage is regulated and remains approximately constant (e.g., by a DC-link chopper or voltage protection scheme) [14], which allows us to focus on the grid-side dynamics independently.

The dynamic behavior of the GFL-inverter is modeled as follows. The state vector $\mathbf{x}$ contains the inverter and grid side currents as well as capacitor voltages in dq-axes. The inputs are the inverter side dq-axes voltages $\mathbf{u}$ and the outputs are the grid side currents $\mathbf{y}$ in dq-axes. We denote the system state

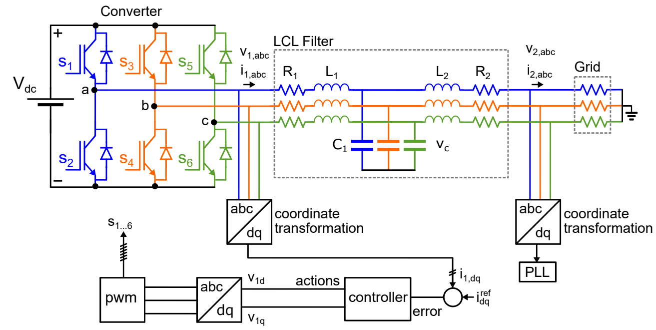

Fig. 1. Grid-connected three phase inverter with LCL filter

by $\mathbf{x} \in \mathcal{X} \subseteq \mathbb{R}^n$, the control inputs by $\mathbf{u} \in \mathcal{U} \subseteq \mathbb{R}^m$, and $\mathbb{R}^+ = \{x \in \mathbb{R} | x \geq 0\}$. The grid following inverter dynamics in the dq-frame are given by a linear state-space model,

$$\dot{\mathbf{x}} = A\mathbf{x} + B\mathbf{u}, \qquad \mathbf{y} = C\mathbf{x} + D\mathbf{u}, \tag{1}$$

where, $\mathbf{x} := [i_{1d}, i_{1q}, i_{2d}, i_{2q}, v_{cd}, v_{cq}]^\top$, $\mathbf{u} := [v_{1d}, v_{1q}]^\top$, and $\mathbf{y} := [i_{2d}, i_{2q}]^\top$. The notations for currents and voltages are labeled in Figure 1 where i_{1d}, i_{1q} are inverter side currents, i_{2d}, i_{2q} are grid-side currents, v_{cd}, v_{cq} are filter capacitor voltages, and A, B, C, and D matrices are derived from the LCL filter parameters and grid angular frequency [15].

The safe current boundary is defined as the maximum RMS or peak current that the inverter can inject into the grid without exceeding its thermal and electrical design limits, thereby ensuring the inverter doesn't get damaged. According to IEEE 1547 standard [16], the inverter must not inject more than 1.1 per unit (pu) of its rated current into the grid. For a three phase system, the safe RMS current that can be injected by the inverter is given by $I_{\text{safe,rms}} = \frac{1.1S}{\sqrt{3}V_{\text{LL,rms}}}$, where, S is the rated nominal power, $V_{\text{LL,rms}}$ is the line to line RMS voltage, and the corresponding safe peak current is $I^{\max} = \sqrt{2}I_{\text{safe,rms}}$.

This paper presents a safe and stable current control problem for grid-following inverters with the control objectives below:

- **Safety Constraint**: Maintain the instantaneous inverter currents (i_{1d}, i_{1q}) within safe limits defined by the current boundary ($i_{1d} \leq i_d^{\max}$, $i_{1q} \leq i_q^{\max}$).
- **Stability Objective**: Ensure asymptotic convergence of inverter currents to their reference values, as far as the safety constraint is satisfied.

III. Safety and Stability via CBFs and CLFs

In this section, we provide the theoretical background and formulation necessary for our methodology, which forms the basis of the CLF–CBF–QP controller developed in Section IV.

Let $\mathcal{X}_{\text{safe}} \subset \mathbb{R}^n$ denote the safe states set, and $\mathbf{x}_g \in \mathcal{X}_{\text{safe}}$ represent the goal state. The objective is to design a control input $\mathbf{u}(t)$ that keeps the system within $\mathcal{X}_{\text{safe}}$ at all times while reaching the goal $\mathbf{x}_g$. A continuously differentiable scalar function $h(\mathbf{x}) : \mathbb{R}^n \to \mathbb{R}$ is called a control barrier function (CBF) if the safe set is its zero-level set, $\mathcal{X}_{\text{safe}} = \{\mathbf{x} \in \mathbb{R}^n \mid h(\mathbf{x}) \geq 0\}$, and $\nabla_{\mathbf{x}} h(\mathbf{x}) \neq 0$ at the boundaries of the safe set

$\mathbf{x} \in \delta\mathcal{X}_{\text{safe}}$. CBFs are a tool to ensure forward invariance of the safe set due to next theorem by Ames et al. [17].

Theorem 1 (Forward Invariance [12])**.** *Consider a control barrier function $h(\mathbf{x}) : \mathbb{R}^n \to \mathbb{R}$ and its safety condition,*

$$\nabla_{\mathbf{x}} h(\mathbf{x})^\top \dot{\mathbf{x}} + \alpha_h(h(\mathbf{x})) \geq 0, \tag{2}$$

where $\alpha_h(\cdot)$ is an extended class-$\mathcal{K}$ function, and if $\mathbf{x} \in \mathcal{X}_{safe} \equiv h(\mathbf{x}) \geq 0$. If the system starts from a safe state, $\mathbf{x}(0) \in \mathcal{X}_{safe}$, and the closed-loop dynamics (1) *evolve under control inputs $\mathbf{u}$ that satisfies* (2)*, then for all future time $t \geq 0$ the state remains safe $\mathbf{x}(t) \in \mathcal{X}_{safe}$, that is, the set $\mathcal{X}_{safe}$ is forward invariant.*

Theorem 1 requires (2) to be satisfied for all $t \geq 0$, but a discrete time controller, in practice, can only guarantee the satisfaction at finite time intervals. Our next theorem lays out the criteria on $\alpha_h(\cdot)$ to ensure safety for switching time Δt_s.

Theorem 2. *A discrete time controller guaranteeing the condition* (2) *of system evolving according to* (1) *will stay safe for small time $\Delta t_s \ll 1$ if, $\alpha_h(z) \leq z/\Delta t_s = z f_s$ for all $z \in [0, h^{max}]$, where $h^{max} := \max_{\mathbf{x} \in \mathcal{X}_{safe}} h(\mathbf{x})$.*

Proof. Assuming $\dot{h}(\mathbf{x}(t))$ to be constant during the small time, we can bound time to collision Δt_c as,

$$\Delta t_c := \int_h^0 \frac{dh(\mathbf{x})}{\dot{h}(\mathbf{x})} \overset{\Delta t \ll 1}{\approx} \frac{h(\mathbf{x}(0))}{|\dot{h}(\mathbf{x}(0))|} \geq \frac{h(\mathbf{x})}{\alpha_h(h(\mathbf{x}))}. \tag{3}$$

Hence, safety can be guaranteed by choosing a switching time less than the worst-case collision time, $\Delta t_s = \frac{1}{f_s} \leq \frac{h(\mathbf{x})}{\alpha_h(h(\mathbf{x}))}$. □

A continuously differentiable scalar function $\nu(\mathbf{x}) : \mathbb{R}^n \to \mathbb{R}^+$ is called a **control Lyapunov function** (CLF) if it encodes the stability and goal-reaching objective and satisfies, $\nu(\mathbf{x}_g) = 0$ and $\nu(\mathbf{x}) > 0 \;\; \forall \mathbf{x} \neq \mathbf{x}_g$. Minimizing the time derivative of $\nu(\mathbf{x})$, $\dot{\nu}(\mathbf{x}, \mathbf{u}) = \nabla_{\mathbf{x}} \nu(\mathbf{x})^\top \dot{\mathbf{x}}$ along the system trajectory encourages the fastest descent of $\nu(\mathbf{x})$ toward zero and guarantees asymptotic convergence to the goal $\mathbf{x}_g$. This can be combined with (2) to achieve stability and safety through the following optimization:

$$\begin{aligned} \mathbf{u}^* &= \arg\min_{\mathbf{u}} \Phi(\mathbf{u}), \text{ s.t. } \nabla_{\mathbf{x}} h(\mathbf{x})^\top \dot{\mathbf{x}} + \alpha_h(h(\mathbf{x})) \geq 0, \\ &\text{where } \Phi(\mathbf{u}) := \nabla_{\mathbf{x}} \nu(\mathbf{x})^\top \dot{\mathbf{x}} + \lambda \|\mathbf{u}\|^2. \end{aligned} \tag{4}$$

Here, $\lambda > 0$ regulates control effort. This formulation yields a control input that minimizes the CLF objective while respecting CBF-enforced safety constraint.

In general, the CBF $h(\mathbf{x})$ may have a higher relative degree, when the control input $\mathbf{u}$ does not show up in the first-order derivative of the barrier function $\dot{h}(\mathbf{x})$, when $\nabla_{\mathbf{x}}^\top h(\mathbf{x}) B = 0$. In such cases, higher-order CBF formulations are required to enforce safety [18], [19]. However, we design CBF to be relative degree one, hence the standard first-order CBF condition (2) is sufficient to guarantee safety, and we focus on this case throughout our analysis.

IV. Methodology

In this section, we develop the safety and tracking objectives for the inverter dynamics in (1). This is achieved by designing a CLF objective, CBF safety constraints, and the corresponding CLF-CBF-QP formulation.

A. Control Lyapunov Function Design

To guarantee asymptotic convergence of the inverter current to its reference, the CLF is defined as:

$$\nu(\mathbf{x}) := (\mathbf{x} - \mathbf{x}^{\text{ref}})^\top P (\mathbf{x} - \mathbf{x}^{\text{ref}}), \tag{5}$$

where $\mathbf{x}^{\text{ref}}$ denotes the reference state $[i_d^{\text{ref}}, i_q^{\text{ref}}]$ and P is the positive-definite matrix obtained from the LQR solution. In the LQR framework, the optimal feedback gain K minimizes the infinite-horizon quadratic cost function:

$$J = \int_0^\infty \left[(\mathbf{x} - \mathbf{x}^{\text{ref}})^\top Q (\mathbf{x} - \mathbf{x}^{\text{ref}}) + \mathbf{u}^\top R \mathbf{u} \right] dt, \tag{6}$$

where $Q \geq 0$ and $R \geq 0$ are the state and control weighting matrices respectively. The matrix P is the unique positive-definite solution to the algebraic Riccati equation: $A^\top P + PA - PBR^{-1}B^\top P + Q = 0$. This ensures that $\nu(\mathbf{x})$ decreases monotonically under the optimal control feedback $\mathbf{u} = -K(\mathbf{x} - \mathbf{x}^{\text{ref}})$.

The gradient of Lyapunov function (5) is $\nabla_{\mathbf{x}} \nu(\mathbf{x}) = 2P(\mathbf{x} - \mathbf{x}^{\text{ref}})$. Substituting linear system dynamics (1) and $\nabla_{\mathbf{x}} \nu(\mathbf{x})$ in objective of (4) and omitting terms independent of $\mathbf{u}$ which do not affect the optimization, we get:

$$\arg\min_{\mathbf{u}} \Phi(\mathbf{u}) = \arg\min_{\mathbf{u}} 2(\mathbf{x} - \mathbf{x}^{\text{ref}})^\top PB\mathbf{u} + \lambda \|\mathbf{u}\|^2. \tag{7}$$

B. Control Barrier Function Design

The safety limits on the inverter currents are ensured using CBFs defined as equations (8). Imposing these safety constraints makes sure that the inverter's d- and q-axis currents always remain within the allowable limits.

$$h_d(\mathbf{x}) := i_d^{\max} - i_{1d} \geq 0, \quad h_q(\mathbf{x}) := i_q^{\max} - i_{1q} \geq 0. \tag{8}$$

Each barrier function h_d and h_q contributes to defining the forward invariant safe set $\mathcal{X}_{\text{safe}}$ as,

$$\mathcal{X}_{\text{safe}} := \{\, \mathbf{x} \in \mathbb{R}^n \mid h_d(\mathbf{x}) \geq 0,\ h_q(\mathbf{x}) \geq 0 \,\}. \tag{9}$$

To guarantee forward invariance of $\mathcal{X}_{\text{safe}}$, the CBF constraint is imposed as equation (2) which ensures the current trajectory always stay within the safe boundary by explicitly tying the inverter voltages (v_{1d}, v_{1q}) to the instantaneous current magnitudes ensuring the currents remain within the safe set.

How to choose α_h? In CBF, the choice of $\alpha_h(\cdot)$ is highly influential and should be chosen carefully. The function α_h can be linear, super-linear, or sub-linear extended class-$\mathcal{K}$ function. A super-linear α_h allows more freedom far away from the unsafe set, but leads to aggressive control near the safety boundary. On the other hand, a sub-linear α_h leads to smoother control at the cost of constrained control even far away from the safe set. We chose a super-linear α_h,

$$\alpha_h(z) := \gamma(z+1)\log(z+1) \le z f_s \quad \forall z \in [0, h^{\max}], \quad (10)$$

where $\gamma \in (0, \frac{h^{\max} f_s}{(h^{\max}+1)\log(h^{\max}+1)}]$. The hyperparameter γ is upper bounded by the safety requirements of a finite-time discrete controller (Theorem 2). To find a reasonable lower bound for γ, we choose states $\mathbf{x}_\mathrm{n}$ for normal operation where CBF constraint must not be active and choose a γ that ensures, $\frac{-\min_{\mathbf{u}} \nabla_{\mathbf{x}}^\top h(\mathbf{x}_\mathrm{n})(A\mathbf{x}_\mathrm{n}+B\mathbf{u})}{(h(\mathbf{x}_n)+1)\log(h(\mathbf{x}_n)+1)} < \gamma \le \frac{h^{\max} f_s}{(h^{\max}+1)\log(h^{\max}+1)}$. For our experiments, we use $\gamma_d = \gamma_q = 6000$.

C. Unified CLF-CBF Control Law

The control input $\mathbf{u}$ is obtained at each timestep by solving the quadratic program (QP):

$$\mathbf{u}^* = \arg\min_{\mathbf{u}\in\mathbb{R}^2} 2(\mathbf{x}-\mathbf{x}^{\mathrm{ref}})^\top PB\mathbf{u} + \lambda||\mathbf{u}||^2 \quad (11)$$
$$\text{s. t.} \quad \nabla_{\mathbf{x}} h_d(\mathbf{x})^\top \dot{\mathbf{x}} + \gamma_d(h_d(\mathbf{x})+1)\log(h_d(\mathbf{x})+1) \ge 0,$$
$$\text{and} \quad \nabla_{\mathbf{x}} h_q(\mathbf{x})^\top \dot{\mathbf{x}} + \gamma_q(h_q(\mathbf{x})+1)\log(h_q(\mathbf{x})+1) \ge 0.$$

The objective penalizes the control effort and Lyapunov function's rate of change. This ensures the control input minimizes the CLF cost while satisfying all CBF constraints.

V. Experiments, Results and Discussion

In this section, we evaluate the proposed CLF-CBF-QP controller for normal conditions and voltage sag events, and compare with the benchmark results obtained from the use of PI with current limiter and LQR controller. The QP (11) is solved to produce the voltage commands $\mathbf{u}^* = (v_{1d}^*, v_{1q}^*)$ for the proposed controller. Simulations are conducted in MATLAB/Simulink 2024b where a 100 kVA grid following inverter connected to a three-phase grid through an LCL filter. Key simulation parameters are listed in Table I.

TABLE I
Simulation Parameters for Grid-Connected Inverter System

Parameter	Value
Rated Apparent Power, S	100 kVA
DC-Link Voltage, V_{dc}	1500 V
Grid Line-to-Line RMS Voltage, V_{LL}	400 V
Grid Frequency, f	60 Hz
Inverter-Side Inductance / Resistance, L_1 / R_1	500 μH / 1 Ω
Grid-Side Inductance / Resistance, L_2 / R_2	150 μH / 1 Ω
Filter Capacitance, C_1	100 μF
Switching Frequency, f_s	10 kHz
Maximum d-Axis Current, $i_d^{\max}$	224.5 A

Baseline: PI and LQR Controllers. To demonstrate the advantages of our controller, we use PI controller with proportional gain $K_p = 6$ and integral gain $K_i = 10000$ as a baseline. Our second baseline is LQR controller where the control input is obtained by minimizing a quadratic cost from equation (6). These controllers lack inverter constraints awareness causing aggressivr response to reference error that cannot be suppressed by LCL filter, leading to current overshoot.

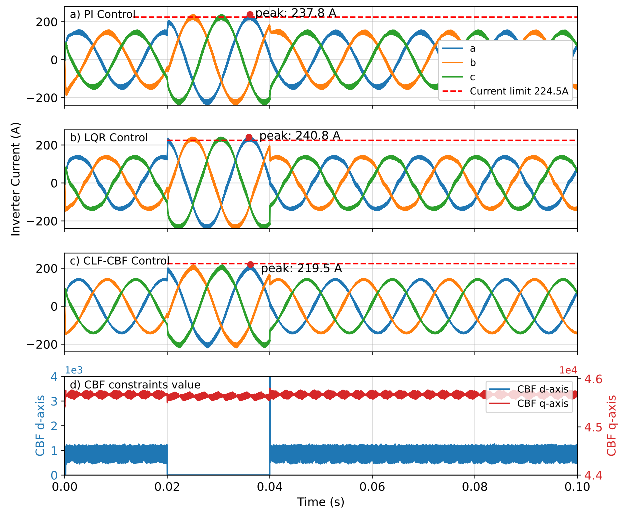

Fig. 2. 3 phase Inverter current for PI with current limiter, LQR, and CLF-CBF based controller for 0.6 pu. voltage sag and CBF for d- and q-axis current

CLF-CBF-QP controller is provably safe and fast. From $I_{\mathrm{safe,rms}}$, the safe current limit is calculated as $i_d^{\max} = 224.5A$. For all controllers, voltage sag of 0.6 pu was introduced at 0.02-0.04 seconds to evaluate transient safety and dynamic recovery. Figure 2 shows the inverter phase current for all three controllers. Figure 2(a) shows PI and (b) LQR controllers exhibited transient current peaks up to $237.8A$ and $240.8A$, respectively, exceeding the safe threshold. In contrast, the proposed CLF-CBF-QP controller successfully restricted the peak to $219.5A$, maintaining the current strictly within the allowable region ($< 224.5A$) as shown in Figure 2(c). This improvement results from the barrier constraint actively regulating the current magnitude to preserve forward invariance of the safe set, even during fast transients. The computation time for solving each QP in unoptimized MATLAB code is ($271.5\mu s$). While our prototype implementation is in Matlab, we conducted preliminary experiments using C++ QP-solver (OSQP [20]), which requires only $3.73{\pm}0.28\mu s$. Using a C++ reimplementation, we can run it at > 250kHz.

CLF-CBF-QP has better transient behavior. Figure 3 illustrates the d-axis current tracking performance under three controllers. During normal operation, all controllers achieved accurate steady-state tracking. But during the voltage sag, the PI controller exhibited overshoot and delayed recovery as depicted by figure 3(a) while the other two controllers recovered quickly as shown in figure 3(b) and (c). Despite similar recovery of the two controllers due to their shared state-feedback structure, only the proposed controller enforces safety constraints. A slight increase in transient ripple was observed attributed to the rapid adjustments of the inverter voltages required to satisfy the CBF constraint; however, this did not affect steady state accuracy or safety compliance.

CLF-CBF-QP has better harmonics. Figure 4 shows the fast Fourier transform (FFT) analysis of the inverter output current. The PI and LQR controllers produced a total harmonic distortion (THD) of 4.72% and 5.63%, respectively, while

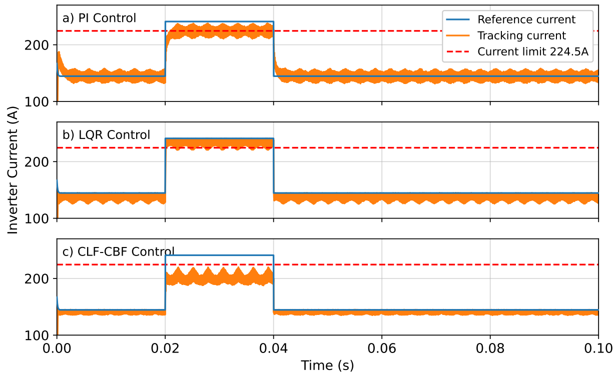

Fig. 3. Reference current tracking for PI with current limiter, LQR, and CLF-CBF based controller for 0.6 pu voltage sag

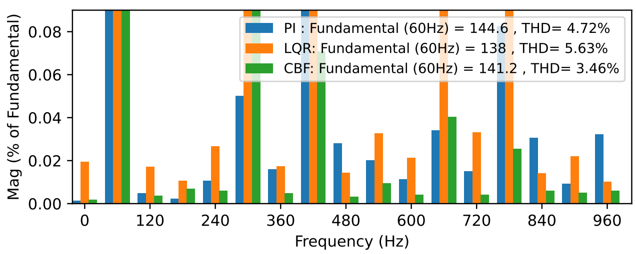

Fig. 4. Harmonic spectrum comparison current under PI, LQR, and CLF-CBF based controller

the proposed controller reduced THD to 3.46%. The optimal regulation of the control commands in the proposed method minimized abrupt switching activity and maintained a smooth current waveform, despite the slightly higher transient ripple observed during dynamic event.

CBF constraints get activated in unsafe conditions. The d- and q-axis constraints of (11) plotted in Figure 2 (d) remained strictly positive throughout the simulation, confirming that the inverter's operating state stayed within the predefined safe set even during the voltage sag. The results verify the controller's effectiveness to limit the inverter current within the safe set without sacrificing stability.

The proposed controller successfully achieved both stability and safety under normal and disturbed grid conditions. Compared to the baseline PI and LQR controllers, it strictly enforced current-limiting constraints during voltage sag, obtained fast transient recovery without overshoot, and improved steady-state harmonic performance. Overall, the results confirm that the CLF-CBF control framework provides a unified approach for safe and effective inverter current regulation.

VI. Conclusion

In this paper, a CLF–CBF-based control framework for safe control of a grid-connected inverter was presented. Unlike conventional schemes that rely on post-hoc current limiting or saturation blocks, the proposed approach embeds analytical safety guarantees directly into the control design. Rigorous analysis based on control barrier and Lyapunov functions is provided to establish formal safety guarantees. Simulation results show that the controller can rigorously enforce current constraints under severe voltage sags, maintaining the inverter current within a prescribed safety boundary while achieving fast transient recovery, reduced harmonic distortion, and robust performance during rapid voltage variations. These results highlight the superior safety-oriented behavior of the proposed controller compared with a conventional rule-based strategy.

References

[1] O. F. Rodriguez-Martinez, J. L. Diaz, O. D. G. Rivera, M. P. Gomez, C. J. D. Munoz, C. A. V. Penagos, A. C. Luna, and F. Andrade, "Centralized secondary control scheme for delay compensation based on smith predictor approach," in *2023 PESGM*, 2023, pp. 1–5.

[2] T. Woldu, C. Ziegler, and M. Wolter, "Fault ride through capability enhancement of grid-connected dfig-based wind power generation during voltage dips," in *2023 IEEE PESGM*, 2023, pp. 1–5.

[3] B. Bahrani, S. Kenzelmann, and A. Rufer, "Multivariable-pi-based *dq* current control of voltage source converters with superior axis decoupling capability," *IEEE TIE*, vol. 58, no. 7, pp. 3016–3026, 2011.

[4] S. A. O. D. Silva, R. A. Modesto, L. P. Sampaio, and L. B. G. Campanhol, "Dynamic improvement of a upqc system operating under grid voltage sag/swell disturbances," *IEEE Trans. Circuits and Systems II: Express Briefs*, vol. 71, no. 5, pp. 2844–2848, 2024.

[5] A. Luna, U. Tamrakar, R. Tonkoski, and S. Hietpas, "Linear quadratic regulator controller to improve transient frequency stability through virtual inertia," in *2020 IEEE Power & Energy Society Innovative Smart Grid Technologies Conference (ISGT)*, 2020, pp. 1–5.

[6] A. Ortega, P. McNamara, and F. Milano, "Design of mpc-based controller for a generalized energy storage system model," in *PESGM*, 2016.

[7] T. Zhao, J. Wang, and M. Yue, "A barrier-certificated reinforcement learning approach for enhancing power system transient stability," *IEEE Trans. Power Systems*, vol. 38, no. 6, pp. 5356–5366, 2023.

[8] T. Joswig-Jones and B. Zhang, "Safe control of grid-interfacing inverters with current magnitude limits," *arXiv preprint arXiv:2409.13890*, 2024.

[9] T. Joswig Jones and B. Zhang, "Optimal control of grid-interfacing inverters with current magnitude limits," in *2024 IEEE 63rd CDC*, 2024, pp. 4623–4628.

[10] H. Cui, X. Lu, K. Qu, G. Song, Y. Chen, and K. Xiahou, "Secure load frequency control of multi-area interconnected power system based on high-order control barrier functions," in *2025 37th Chinese Control and Decision Conference (CCDC)*, 2025, pp. 1299–1303.

[11] M. Schneeberger, S. Mastellone, and F. Dörfler, "Safety filter for limiting the current of grid-forming matrix modular multilevel converters," 2025.

[12] A. D. Ames, S. Coogan, M. Egerstedt, G. Notomista, K. Sreenath, and P. Tabuada, "Control barrier functions: Theory and applications," in *2019 18th ECC*. IEEE, 2019, pp. 3420–3431.

[13] K. P. Tee, S. S. Ge, and E. H. Tay, "Barrier lyapunov functions for the control of output-constrained nonlinear systems," *Automatica*, vol. 45, no. 4, pp. 918–927, 2009.

[14] J. Conroy and R. Watson, "Low-voltage ride-through of a full converter wind turbine with permanent magnet generator," *IET Renewable Power Generation*, vol. 1, pp. 182–189, 2007.

[15] S.-J. Yoon, N. B. Lai, and K.-H. Kim, "A systematic controller design for a grid-connected inverter with lcl filter using a discrete-time integral state feedback control and state observer," *Energies*, vol. 11, no. 2, 2018.

[16] IEEE, "Ieee standard for interconnection and interoperability of distributed energy resources with associated electric power systems interfaces," *IEEE Std 1547-2018*, pp. 1–138, 2018.

[17] A. D. Ames, J. W. Grizzle, and P. Tabuada, "Control barrier function based quadratic programs with application to adaptive cruise control," in *53rd IEEE CDC*. IEEE, 2014, pp. 6271–6278.

[18] Q. Nguyen and K. Sreenath, "Exponential control barrier functions for enforcing high relative-degree safety-critical constraints," in *2016 American Control Conference (ACC)*. IEEE, 2016, pp. 322–328.

[19] V. Dhiman, M. J. Khojasteh, M. Franceschetti, and N. Atanasov, "Control barriers in bayesian learning of system dynamics," *IEEE Transactions on Automatic Control*, vol. 68, no. 1, pp. 214–229, 2023.

[20] B. Stellato, G. Banjac, P. Goulart, A. Bemporad, and S. Boyd, "OSQP: an operator splitting solver for quadratic programs," *Mathematical Programming Computation*, vol. 12, no. 4, pp. 637–672, 2020.